

Y-nano X-micro technologies: nanometric optical control

D. W. de Lima Monteiro*, F. P. Honorato*, A. I. Ferreira Jr.*,
O. Soloviev**, G. Vdovin** and M. Loktev**

* OptMA^{lab}, Department of Electrical Engineering, Universidade Federal de Minas Gerais
Av. Antônio Carlos, 6627, 31270-010 Belo Horizonte-MG, Brazil, davies@ufmg.br

** EI Lab., Delft University of Technology, The Netherlands, gleb@titus.et.tudelft.nl

ABSTRACT

Nanometric control of optical quality is relevant in many different fields, ranging from Ophthalmology to Lithography, where ordinary setups suffer from optical aberrations. Most common aberrations feature amplitudes in the nanometer range and are often mapped within apertures on the order of micrometers to centimeters. Compensation of these distortions demand devices with structural resolution that is nanometric in the vertical direction (Y-nano) and micrometric on the horizontal plane (X-micro).

This paper focuses on our recent research progress on wavefront detection and correction, involving sensors, actuators and static components fabricated in the scope of standard Silicon technologies. It also introduces concepts for the homogeneous and smooth texturization of solar cells.

Keywords: adaptive optics, deformable mirror, wavefront sensor, mems, solar cell

1 INTRODUCTION

The demand on optical quality is translated as the maximum acceptable deviation of a given profile. The required accuracy is usually indicated in terms of the wavelength λ and ranges from $\lambda/4$ to $\lambda/1000$, depending on how stringent the application is. Optical aberrations caused either by imperfection in system components or by the propagation media can affect optimal performance of applications such as retinal imaging, astronomical observation through atmospheric turbulence, free-space optical communications and confocal microscopy. This happens because nanometric distortions on a wavefront profile result in degradation of parameters as sharpness, power and resolution.

Adaptive Optics (AO) offers the possibility to restore the original wavefront, but traditional AO components, such as deformable mirrors and wavefront sensors, are either expensive or slow. This has driven research centers to develop affordable devices supposed to attend for dynamic sensing and compensation of aberrations in fast changing systems.

Since most common aberrations feature nanometric amplitudes and are often mapped within apertures on

the order of micrometers to centimeters, suitable adaptive optical devices should preferably bear nanometric vertical resolution and micrometric horizontal resolution, which incidentally are structural characteristics prevailing in microelectronics and micromachining technologies. These technologies have long been capable of reproducing nanometric features in the vertical direction (thin films, membranes and cavities), which suit well for wavefront manipulation - by reflection or transmission - in wavelengths within and close to the visible spectrum ($\sim 380\text{nm} - 750\text{nm}$). The maturity and availability of these processes yield a range of reliable, integrated and potentially inexpensive devices for wavefront restoration in industrial, scientific and medical systems.

The following sections report on recent results of micromachined adaptive correctors, CMOS wavefront sensors, liquid-crystal adaptive optics with modal response, sub-nanometric profile sensor for next-generation EUV mirrors and bulk micromachined aspherical surfaces. Insights on solar-cell technology with inexpensive micrometric texturization are also presented.

2 MEMS MIRROR

A conducting membrane clamped around its perimeter and suspended above an array of electrodes can be electrostatically deflected downwards if one applies a potential difference between it and the electrodes. The membrane profile can be modulated by applying an appropriate voltage to each electrode [1]. Therefore, upon reflection, a distorted wavefront $W(x, y)$ can be converted back to a plane wavefront if the membrane shape is $W(x, y)/2$.

The membrane has to be smooth, resistant and stretched, which is achieved by depositing a thin tensile stressed Si_nN_m mechanical layer ($\sim 300\text{nm}$ to 800nm) on a silicon substrate. Si_nN_m has very good mechanical properties, is not brittle and is compatible with microelectronic fabrication processes; deposition by LPCVD (Low-Pressure Chemical Vapor Deposition) guarantees a highly pure and uniform layer. The membrane is released by back anisotropic etching of bulk silicon. If anisotropic etching with a high selectivity is used (e.g.: KOH aqueous solution to etch a $< 100 >$ wafer), the nitride membrane is kept

unaffected by the etching of the silicon substrate. A circular contour can be stepwise approximated by designing the etch window as a gear-wheel.

The number of electrodes range so far from 1 to 119 and the membrane sizes from 5 to 50mm. Deflection of the membrane is proportional to the voltage squared, where the control voltage can reach up to 300V.

To ensure reflectivity and conductivity, the membrane is coated with a 200nm aluminum or gold layer. These coatings are sufficient for a broad spectral range in the visible (Al) and the infrared (gold) regions. Coating the membrane with a Cr/Ag layer plus a dielectric stack can result in close to 100% reflectivity in a narrow wavelength window.

Non-micromachined deformable mirrors we have fabricated are based on the deflection of a plate in mechanical contact to the actuators. These are either piezo rods, which elongate under a potential difference; or resistors [2], which elongate under current flow.

3 LC MODAL CORRECTOR

The birefringence of a continuous Liquid-Crystal (LC) layer can be controlled by applying an electric field across it. The consequent polarization change of the LC molecules modulates the light phase of a beam propagating through it.

An LC layer is placed between a transparent top electrode (ITO) and a continuous resistive layer (sheet resistance $\sim 0.1\text{-}1\text{M}\Omega/\text{sq}$). AC control voltages are applied to metal nodes distributed over the resistive layer, which is coated with a reflective dielectric film. The smooth voltage variation on the resistive layer ensures smooth phase modulation of the incoming beam. A *mode* is the polarization state of the layer caused by actuation of a single node [3]. Wavefront modal control, resulting from the combination of several modes, requires much less electrodes than zonal control, in which zones are defined by independent LC chambers (pixels).

Despite the relatively slow LC response times (typically hundreds of ms), LC phase modulators represent a feasible and inexpensive alternative to deformable mirrors because of some particularly attractive characteristics as large amplitude of the controllable phase-delay (tens of wavelengths), low power consumption ($0.1\text{ mW}/\text{cm}^2$), absence of moving parts and low control voltages. These features suit well the concept of implantable adaptive lenses in the human eye [4], which can be controlled remotely by coil coupling.

A particular feature that distinguishes modal LC wavefront correctors from deformable mirrors is the possibility to drive each actuator with several degrees of freedom: amplitude, frequency and phase of the AC control voltage. The combination of amplitude and phase modulation (fixed frequency) has proven to yield the

best wavefront correction, minimizing phase spikes at the locations of the metal nodes.

Integration of a driver circuit with an LC corrector, in a standard silicon process, is fully feasible because of voltage compatibility and absence of micromachining steps. We designed a grid of 39 concentric Al/Si electrodes connected to metal pads at the periphery of the chip. Manufacturing the resistive layer with a sheet resistance in the range of $\sim 0.1\text{-}1\text{M}\Omega/\text{sq}$ pose one of the main technical problems. Thin films of n-type doped silicon carbide were deposited using PECVD (Plasma Enhanced Chemical Vapor Deposition) and then annealed with an excimer laser (UV range). However, patterning this layer and the layers above with no damage to its conductive properties are yet to be solved. Alternatively, it is possible to combine zonal and modal approaches by replacing a continuous resistive layer by a network of discrete IC resistors fed by multiplexed metal nodes. Simulation results of these “active electrodes” favor its implementation.

4 CMOS WAVEFRONT SENSOR

Before wavefront compensation takes place, one needs means to track the distortion footprints. In a spectrum of techniques based on interferometry, geometrical optics and irradiance variations, the Hartmann method stands out as one of the most used wavefront sensing techniques. A light beam is sampled into several sub-beams, by an opaque mask with openings, and projected on a screen. When the wavefront is flat the resulting light spots on the screen are located perpendicularly under their respective originating openings. This pattern of light spots is recorded as a reference grid. When a distorted wavefront is sampled, the positions of the spots might not coincide with their reference grid points. The distances are geometrically proportional to the local wavefront tilts, from which the wavefront shape can be evaluated.

A Hartmann-Shack (HS) wavefront sensor replaces the opaque mask with a microlens array. This improves light-collection efficiency, reduces sampling aliasing and prevents intensity variation within sub-apertures from conveying displacement information.

We fabricated an integrated HS wavefront sensor in a $1.6\ \mu\text{m}$ CMOS technology, where a two-dimensional array of 64 optical position-sensitive detectors (PSDs) yield a straightforward computation for the displacements [5]. The chip accommodates both digital and analog circuitry. Each PSD is $600\ \mu\text{m}\times 600\ \mu\text{m}$ large and its response to spot displacements depends on the spot profile and on the ratio of the effective radius to the PSD lateral size.

This sensor requires spots on the order of μW , operates at 3kHz and features a very good position

resolution ($1\mu\text{m}$); therefore a good wavefront accuracy ($\sim 13\text{nm}$ @ $10\mu\text{W}/\text{spot}$). We now target new pixel layouts in standard CMOS that exploit the limits of design rules to pursuit comparable resolution @ $10\text{nW}/\text{spot}$. CMOS wavefront sensors can, in principle, profit from a hardware-based neural network for wavefront reconstruction on chip, eliminating the computer as the processor unit.

A neural network would attempt to identify the best decomposition of an arbitrary optical aberration into a set of known functions. The approximation accuracy depends on the sensor sampling capabilities and on the number and type of the input functions. An insufficient number of functions might lead to an incomplete representation of the target aberration, whereas a too large set of function is prone to introducing residual approximation errors.

A simple algorithm that can be used to approximate an optical aberration composed of the sum of three known functions, could assume an Adaline [6] architecture with three inputs and one output and the following specifications: the gradient convergence rate η should be 0.01 to guarantee a smooth convergence and the approximation error is made smaller than $1\text{e-}6$ to minimize influences of the algorithm in the optical approximation. Each input contains the sensor response to a pre-defined optical aberration. The algorithm outputs a weighted sum of the input values in an attempt to minimize its deviation from an arbitrary response measured by the sensor.

5 EUV-MIRROR PROFILOMETER

There exists already a demand for optical components with a profile accuracy in the angstrom range (\AA). One of the approaches to next generation lithography will be based on Extra Ultra Violet light (EUV - $\lambda = 11\text{nm}, 13\text{nm}$), which requires extremely precise projection mirrors. Our challenge is to construct a device able to measure the profile of such a mirror with an accuracy down to 1 angstrom over surface-amplitude variations up to 3 mm.

Conventional interferometric methods are not applicable to this purpose. The idea is to couple two measurement steps: measurement of millimeter amplitudes with low accuracy and measurement of sub-micron amplitudes with sub-nanometric accuracy [7]. To achieve the latter we rely on the conversion of optical path differences into temporal phase differences of low-frequency amplitude-modulated optical signals (1...100 kHz). The profile accuracy then depends on the precision of the phase sensor. It was shown that the phase should be measured over an array of at least 24×24 photodetectors with $2\pi/10^4$ rad precision. In general, photodetectors with very small areas are required, implying pA photocurrents.

We calculate the arctan of phase as the ratio of two values derived from a signal sampled 4 times over a period. The precision increases with the number of measurements, which is limited by the stability of the laser ($\sim 1\text{s}$). To achieve angstrom profile accuracy the sensor must be able to detect the phase of a 10kHz modulated laser with an accuracy of 10^{-4} during 1s. The sensor accuracy can be improved by the continuous multiplication of the signal by a reference function (e.g. sinusoidal signal, pulse signals).

We designed the pixel structure in the framework of standard CMOS technology, where we exploit the subthreshold region of operation of the MOSFETs in translinear multiplier circuits to be able to handle the small generated photocurrents effectively.

6 MACHINING OF ASPHERICS

Machining of aspherical surfaces in Silicon has not yet blossomed due to the previous lack of an inexpensive and reproducible technique. Arbitrary smooth surfaces with low aspect ratios might prove useful complementing current MEMS devices fabricated by either bulk or surface micromachining.

Aspherics with nanometric profile relief and micrometric lateral dimensions can be very useful in Optics, and the processed Si substrate can be either used as a mirror or as a mould to custom phase plates. There are various applications in which aspherical micro-optics can be employed, e.g. optical telecommunications, beam forming optics, hybrid wavefront sensors, beam shaping and displays.

We developed a method, based on anisotropic etching of bulk silicon, in which we approximate arbitrary surfaces by laterally overlaying $N \times N$ hemispherical cavities with different sagittae (depths) and diameters [8]. The sagitta s of each cavity is proportional to the size of the respective initial opening d_0 on the oxide mask: $s = \alpha d_0$, where α is a parameter that depends on the etch ratio between different crystallographic planes, on the etchant concentration and on the etching temperature. This method relies on the fact that a $\langle 111 \rangle$ -faced pyramidal pit KOH-etched on a $\langle 100 \rangle$ surface evolves into a smooth hemispherical cavity if one etches the whole surface long enough [9], as depicted in Fig. 1.

We produced a number of 1-mm and 5-mm phase plates that replicate a number of typical optical aberrations: tilt, defocus, astigmatism, spherical aberration and higher order terms. These plates can be used for the compensation of static custom aberrations. This technology requires a single lithographic mask to create the initial pyramidal pits and only two etch steps, which makes it suitable for serial production of high-quality reflective and refractive components.

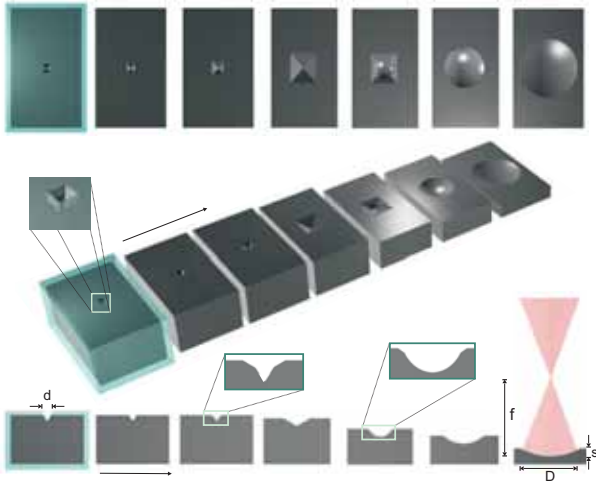


Figure 1: Hemisphere resulting from maskless etching.

7 SOLAR-CELL TEXTURIZATION

The inexpensive single-mask anisotropic etching of shallow hemispherical cavities can be used to mould the substrate of silicon solar cells to maximize the surface area exposed to the sun while uniformizing the conversion efficiency for a broad range of solar angles.

Nowadays, large-scale deployment of solar cells is still primarily limited by the low efficiency of low-cost solar cells. The solar cell efficiency depends on the semiconductor, the fabrication technology, the cell structure and on whether the cell is crystalline, polycrystalline or amorphous. Silicon is an appropriate material because of its abundancy, mature processing technology, mechanical strength and spectral sensitivity coincident with the region of maximum power of the solar spectrum. P-N and P-I-N photosensitive structures fabricated with amorphous silicon yield the lowest production costs. Their efficiency depends on the homogeneity and uniformity of the amorphous silicon (a-Si) films and on the texturization of the substrate where the films are deposited.

The best conversion efficiency is achieved when the incoming light rays are perpendicular to the cell. An existing texturization technique consists in populating the cell surface with pyramidal pits. Pyramids, however, only favor optimal incidence for two angles of solar inclination (two opposed faces of the pyramid) [10], and are prone to shading. Hemispheric depressions, on the other hand, do not yield additional costs as compared to the previous methods, can feature 100% fill factor and favors a larger efficiency uniformity for oblique solar reception. Besides, the cell itself can serve as a perfect mould to replicate inexpensive solar concentrators in polymer.

For every three hundred cells, of any given size, the gain in surface area can be that of one extra cell if the surface is texturized with micrometric cavities. The

maximum gain depends on the cavity diameter, which recursively depends on the initial parameter of the proposed technology.

8 CONCLUSIONS

Fabrication technologies with nanometric vertical resolution and micrometric lateral resolution are suitable for the implementation of devices and components used to control nanometric features in optical systems. Devices for wavefront detection and control in the framework of silicon microtechnologies, as well as solar cells with controlled smooth texturization can be fabricated. Low-cost, integrability and reproducibility are some of the most poignant advantages.

ACKNOWLEDGMENTS

The authors are thankful to the Dutch Technical Foundation (STW).

REFERENCES

- [1] G. Vdovin et al., "Technology and applications of micromachined silicon adaptive mirrors," *Optical Engineering* **36**, p.1382-1390, 1997
- [2] G. Vdovin et al., "Deformable mirror with thermal actuators," *Optics Letters* **27** (9), p.677-679, 2002
- [3] A. F. Naumov et al., "Liquid-crystal adaptive lenses with modal control," *Optics Letters* **23** (13), p.992-994, 1998
- [4] G. Vdovin et al., "On the possibility of intraocular adaptive optics," *Opt.Express*, **11** (7), p.810-817, 2003
- [5] D. W. de Lima Monteiro et al., "High-speed wavefront sensor compatible with standard CMOS technology," *Sensors and Actuators A*, **109** (3), p.22-230, 2004
- [6] B. Widrow et al., "Perceptrons, Adelines and Back-propagation," *The Handbook of Brain Theory and Neural Networks*, Ed. Arbid, MIT Press, Cambridge, p.719-724, 1995
- [7] O. Soloviev et al., "Implementations of Phase Sensitive Detectors for Heterodyne Interferometer," *Proc. Eurosensors XVI*, Prague, p.681-684, 2002
- [8] D. W. de Lima Monteiro et al., "Single-mask microfabrication technology of aspherical optics using KOH anisotropic etching," *Opt. Express* **11** (18), p.2244-2252, 2003
- [9] D. Kendal et al., *Opt. Eng.* **33** (11), p.3578-3588, 1994
- [10] M. Lipinski et al., "The Industrial Technology of Crystalline Silicon Solar Cells," *J. Optoelectronics and Advanced Materials*, **5** (5), p.1365-1371, 2003